Scattering of x rays by the bound and free electrons in dense plasma

Eran Nardi
Department of Nuclear Physics, The Weizmann Institute of Science, Rehovot, Israel
(Received 16 July 1990)

We present a method for calculating the total x-ray-scattering cross section as a function of angle for kilo-electron-volt x rays scattered by partially ionized hot dense plasma. The calculational procedure is based on determining the separate contributions of bound and free electrons to the scattering cross sections. Basic distributions needed for the calculation are obtained by solving the Thomas-Fermi model in the correlation sphere, where both electrons and ions are accounted for. The results indicate significant changes in the intensity and angular distribution of the scattering cross sections between different plasma conditions and between plasma and cold material.

INTRODUCTION

The subject of this paper is the calculation of the scattering of kilo-electron-volt x rays from hot dense plasma. This topic is of recent interest due to the development and study of x-ray lasers and of their interaction with matter as well as to the possibility of using x rays in order to diagnose dense hot plasma.[1] In the latter respect we note that recent experiments using coalescing shock waves generated with intense laser beams[2] have produced plasmas which could give very distinct angular distributions of scattered x rays (see the following). The scattered x-ray spectrum is not treated here, but rather the intensity of the scattered radiation as a function of angle. Theoretical work which deals with the spectrum for completely ionized dense plasmas has been carried out by Theimer[3] and more recently by Boercker *et al.*[4] A preliminary account of the work to be described in this paper has recently been published by us.[5]

The total x-ray-scattering cross-section calculation is based here on determining the separate contributions of the free and bound electrons and the interference between both these contributions as derived by Chihara[6] for the case of liquid metals. The similarity between plasmas and liquid metals was first pointed out by Deutsch[7] and more recently by Chihara.[8] In this context it is noted that the x-ray-scattering cross section in liquid metals is strongly influenced by the ion structure factor[9] and this effect manifests itself clearly in the plasma calculations performed here.

In the second section the basic formulas describing the x-ray scattering are derived. The third section deals with the methods employed for solving the plasma physics problem, whereby the basic physical distributions needed for the cross-section calculation are derived. Following this we discuss the calculation of the incoherent scattering cross section of the bound electrons of the partially ionized plasma treated here, as well as the scattering from the free electrons. Results are given in the fifth section for Fe plasma at 150 eV at the natural density, and for carbon plasma at 13 eV and a density of 5.4 g/cm^3 as well as for carbon at 2 eV and 0.1 g/cm^3 and for fully ionized high-temperature carbon. The first two carbon plasmas are of special interest as they could be produced in current laboratory experiments.[2]

BASIC FORMULAS

The derivation of the coherent and incoherent scattering cross sections presented below is due to Chihara, who derived them for liquid metals.[6] Basic to the method is the separation between bound and free electrons. The same cross sections were also recently derived by Oliva and More[1] for plasma. The basic relation for the scattering of radiation by the electrons is given by

$$I(Q)=I_{\rm cl}(Q)\left\langle \left| \sum_{k=1}^{K} \exp(iQr_k) \right|^2 \right\rangle \tag{1}$$

where the brackets denote a ground-state average and Q is the momentum change induced by the scattering process, r_k is the position coordinate of the kth particle, and $I_{\rm cl}(Q)$ is the classical Thompson scattering cross section. We use the definition

$$\rho_e(Q)=\sum_{k=1}^{K} \exp(iQr_k) \ . \tag{2}$$

Assuming a total of K electrons and N ions, denoting by Z_f the number of free electrons per ion and by Z_b the number of bound electrons per ion, we write

$$K=Z_fN+Z_bN \ .$$

According to the well-accepted procedure of dense plasma physics and using Chihara's derivation for liquid metals we separate between the contributions of the free and bound electrons. Thus, $\rho_b(Q)$ is the sum in Eq. (2) for bound electrons while $\rho_f(Q)$ is this sum for the free electrons. We therefore obtain

$$\begin{aligned} &\rho_e(Q)=\rho_b(Q)+\rho_f(Q) \ , \\ &\langle|\rho_e(Q)|^2\rangle=\langle|\rho_b(Q)|^2\rangle+\langle|\rho_f(Q)|^2\rangle \\ &\qquad\qquad +2\langle|\rho_b(Q)\rho_f^*(Q)|\rangle \ . \end{aligned} \tag{3}$$

The first and second terms give bound- and free-electron scattering, respectively, while the last term is an interference term. Denoting the position of ion α by R_α and the electron bound to this ion by $r_{j\alpha}$, the next step is to replace r_k for the bound electrons in Eq. (3) with $R_\alpha + r'_{j\alpha}$. We quote the results of this procedure as carried out by Chihara[6] and write for the bound-electron term

$$\langle |\rho_b(Q)|^2 \rangle = N|f_{\rm I}(Q)|^2 S_{\rm II}(Q) + NZ_b S^{\rm I}_{\rm inc} \tag{4}$$

where $f_{\rm I}(Q)$ is the bound-electron form factor and with $n_b(r)$ the bound-electron charge density it is defined by

$$f_{\rm I}(Q) = 4\pi \int n_b(r) \frac{\sin Qr}{Qr} r^2 dr \ . \tag{5}$$

$S_{\rm II}(Q)$ is the ion-ion static structure factor given by

$$S_{\rm II}(Q) = \sum_{\alpha,\beta} \langle \exp[iQ(R_\alpha - R_\beta)] \rangle$$
$$= 1 + \bar{n}_{\rm I} \int h_{\rm II}(r) \frac{\sin Qr}{Qr} r^2 dr \tag{6}$$

where $h_{\rm II}(r) = g_{\rm II}(r) - 1$, with $g_{\rm II}(r)$ the two-particle radial distribution function. $\bar{n}_{\rm I}$ is the asymptotic (average) ion density. $S^{\rm I}_{\rm inc}$ is the incoherent scattering factor of the bound electrons and it is given by

$$S^{\rm I}_{\rm inc} = \frac{1}{Z_b} \left[\sum_{i,j} \langle \Psi_0 | \exp[iQ(r_i - r_j)] | \Psi_0 \rangle - |f(Q)|^2 \right] . \tag{7}$$

The details of the derivation of this term will be given below.

The free-electron term appearing in Eq. (3) is Z times the static electron-electron structure factor of the free electrons $S_{ee}(Q)$; this term will also be discussed below.

The interference term is

$$2\langle \rho_b(Q) \rho_f^*(Q) \rangle = 2 f_{\rm I}(Q) S_{e{\rm I}}(Q) \tag{8}$$

where $S_{e{\rm I}}(Q)$ is the free-electron–ion static structure factor, and is given by

$$S_{e{\rm I}}(Q) = 1 + (n_e \bar{n}_{\rm I})^{1/2} \int h_{e{\rm I}}(r) \frac{\sin Qr}{Qr} 4\pi r^2 dr \tag{9}$$

where $h_{e{\rm I}} = g_{ei}(r) - 1$, and $g_{ei}(r)$ is the free-electron–ion radial distribution function.

In summary, the total scattering cross section as a function of the momentum change Q is given by

$$I(Q) = I_{\rm cl}(Q)[|f_{\rm I}(Q)| S_{\rm II}(Q) + 2 f_{\rm I}(Q) S_{e{\rm I}}(Q) + Z_b S^{\rm I}_{\rm inc} + Z_f S_{ee}(Q)] \ . \tag{10}$$

The basic quantities required for calculating the cross section given in Eq. (10) are the bound-electron charge density $n_b(r)$, the static ion-ion structure factor $S_{\rm II}(Q)$, and the free-electron–ion structure factor $S_{e{\rm I}}(Q)$. The bound-electron charge density is needed for the calculation of the form factor $f_{\rm I}(Q)$ and the bound incoherent structure factor $S_{\rm inc}$. The derivation of these is discussed in the following section. As noted the derivation of $S_{ee}(Q)$ is also discussed below.

THOMAS-FERMI CALCULATION IN THE CORRELATION SPHERE

The three basic quantities needed for the calculation of the x-ray-scattering cross section, $n_b(r)$, $S_{\rm II}(Q)$, and $S_{e{\rm I}}(Q)$, were obtained by solving the Thomas-Fermi equation in the so-called correlation sphere. The volume of this sphere contains a large number of ions sufficient to ensure that the ion-ion pair distribution is unity at sufficiently large distances from the central ion situated at the origin.

The two equations of the Thomas-Fermi method in the correlation sphere are the Poisson equation and the equation describing $\rho(r)$, the total charge density which includes electrons with Fermi-Dirac statistics and ions of charge Z^* which possess a given ion-ion radial distribution function $g_{\rm II}(r)$, which together with Z^* must be determined self-consistently. The radius of the correlation sphere is denoted by r_0. We write

$$\nabla^2 V(r) = -4\pi\rho(r) \ , \tag{11}$$

$$\rho(r) = -\left[\frac{8\pi e}{h^3}\right] \times \int_0^\infty p^2 dp \left[\exp\left[\frac{-\mu + p^2/2m - eV(r)}{kT} \right] + 1 \right]^{-1} + Z^* e \bar{n}_{\rm I} g_{\rm II}(r) \ . \tag{12}$$

Changing the variables one obtains the following equation, which differs from the conventional Thomas-Fermi equation in the term $bg_{\rm II}(r)$, which also includes the effective ionic charge Z^*:

$$\Phi''(x) = ax\{I_{1/2}[\Phi(x)/x] - bg_{\rm II}(r)\} \ , \tag{13}$$

where

$$\Phi(x) = [\mu + eV(r)]r/kTr_0, \quad x = r/r_0, \quad a = (r_0/c)^2 \ ,$$
$$1/c = 4\pi e (2m)^{3/4} (kT)^{1/4}/h^{3/2} \ ,$$
$$b = Z^* \bar{n}_{\rm I} e h^3 / 8\pi\sqrt{2}(mkT)^{3/2}$$

with boundary conditions

$$\Phi'(1) = \Phi(1) \ ,$$
$$\Phi(0) = Ze^2/kTr_0 \ .$$

The numerical methods employed in solving Eq. (13) are given in detail in Ref. 10. Solving Φ and thus the potential gives the number of bound electrons and thus Z^*; see Ref. 10. The new value of Z^* is inserted in Eq. (13) together with the modified radial distribution function and the equation is solved once more; this process continues until convergence.

The problem at hand is the method of calculating Z^* and the ion-ion radial distribution function for the plasmas treated here. The case of an Fe plasma at 150 eV and at the natural density has been treated in a preliminary version of this work.[5] This plasma is amenable to a solution using the hypernetted-chain (HNC)–Thomas-

Fermi (TF) method, discussed in detail in Ref. 10. This procedure is based on the self-consistent coupling between the Thomas-Fermi and HNC methods. Unfortunately the HNC–Thomas-Fermi procedure does not converge for the lower-temperature carbon plasma studied in the present paper.

In the case of the lower-temperature plasma the radial distribution function is assumed to be given by the one-component-plasma (OCP) model and is held fixed throughout the calculation. The plasma coupling parameter is given by

$$\Gamma=(Z^*e)^2/kTr_t$$

where

$$r_t=\left[\frac{3}{4\pi}\frac{1}{\bar{n}_1}\right]^{1/3}.$$

Γ is determined from the initial guess of Z^*. The ionic charge Z^* is then determined self-consistently from the solution of Eq. (13). The change in the final value of Z^* relative to the initial guess of Z^* in our calculation has little effect on ion radial distribution function. The OCP assumption, which is tested below for the 150-eV Fe case, could be improved upon in the future but for the purpose of our calculation this assumption is sufficiently accurate.

INCOHERENT SCATTERING FACTOR FOR BOUND ELECTRONS

The incoherent scattering factor of the bound electrons $S_{\rm inc}$ is given in Eq. (7). Mendelsohn and Biggs,[11] who extended the Heisenberg derivation, discussed in detail the computation of the incoherent scattering factor. The dense plasma calculations of the present paper require the incoherent scattering factors from the bound electrons of partially ionized atoms.

The Heisenberg evaluation of $S_{\rm inc}$ is based on antisymmetrized single-particle wave functions. The orbitals are plane waves with momentum values at radius r, ranging from 0 to $P_F(r)$ given by

$$P_F(r)=\frac{h}{2}\left[\frac{3}{\pi}\right]^{1/3}\rho^{1/3}(r),$$

while the incoherent scattering factor for any local electron gas approximation is

$$S_{\rm inc}(Q)=1-\frac{1}{Z_b}\left[\frac{8\pi}{3h^3}\right]\int_0^{r_1}dV\left[P_F(r)-\frac{Qh}{4\pi}\right]^2\times\left[P_F(r)+\frac{Qh}{8\pi}\right], \quad (14)$$

with

$$P_F(r_1)=Qh/4\pi .$$

Tabulations of cross sections of incoherent scattering of atoms at standard conditions were performed using Eq. (14) within the framework of the Thomas-Fermi approximation.[12] The solution of Eq. (13) gives the bound-electron charge distribution (see Ref. 5). Inserting this in Eq. (14) gives the bound-electron incoherent scattering factor. We note that Oliva and More[1] used the Hartree model, which requires the knowledge of the electron wave functions, in order to calculate the incoherent scattering factor.

FREE-ELECTRON SCATTERING

The free-electron scattering term appearing in Eq. (3) is Z_f times the free-electron–electron structure factor $S_{ee}(Q)$. The weak-coupling result for the one-component electron system is given in the Debye limit by the well-known relation

$$S_e(Q)=Q^2/(Q^2+k_e^2) \quad (15)$$

where k_e is the electron Debye length.

For a two-component system of electrons and ions Boercker and More[13] show that, assuming weak coupling,

$$S_{ee}(Q)=S_e(Q)+Z_fS_{\rm II}(Q)[k_e^2S_e(Q)/Q^2]^2 . \quad (16)$$

The same result was obtained by Salpeter.[14] Assuming the electrons and ions are described by the Debye-Hückel theory $S_{ee}(Q)$ reduces to

$$S_{ee}(Q)\equiv(Q^2+k_i^2)/(Q^2+k_i^2+k_e^2) \quad (17)$$

where k_i is the ion Debye length.

In the results given below $S_{ee}(Q)$ plays a prominent role only in the case of the high-temperature completely ionized weakly coupled C plasma (temperature 200 eV, density 0.1 g/cm^3) treated here. $S_{ee}(Q)$ written in the form of Eq. (17) is valid in this case. In the other cases dealt with in the present study, free-electron scattering plays only a minor role in the total cross-section result. This is due to the significant number of bound electrons which dominate the scattering cross sections. The free-electron scattering in these cases was therefore assumed to be given by the Debye-Hückel limit, Eq. (17). A more accurate form of the free-electron scattering using Eq. (16) or even higher-order terms[13] would have only a minor effect on the calculated cross sections.

RESULTS

The x-ray-scattering cross section was calculated using Eq. (10) for iron and carbon plasmas. In the case of iron the plasma was at a very high temperature of 150 eV with the plasma density at 7.59 g/cm^3. For carbon lower-temperature plasmas, which could be currently produced in the laboratory, as well as a high-temperature fully ionized plasma, were studied. In one case the plasma temperature was 13 eV and the density 5.4 g/cm^3 while in the second case treated these values were 2 eV and 0.1 g/cm^3, respectively, while in the fully ionized plasma the temperature was 200 eV and the density 0.1 g/cm^3.

The results for Fe at 150 eV were given in detail in Ref. 5; the solution of Eq. (7) was carried out by the HNC-TF method.[10] The results presented here differ only with respect to the electron-electron structure factor S_{ee} which

was calculated incorrectly in Ref. 5.

In Fig. 1 is plotted the total x-ray-scattering cross section as a function of angle for the iron plasma discussed above, compared to the scattering cross section for cold iron at the natural density assuming no correlation between the atoms. The incident x-ray energy is 10 keV for all the results of Fig. 1. The scattering cross section for a gas of N uncorrelated atoms is given by

$$I(\theta)=I_{\rm cl}(Q)N[\,|f_A(Q)|^2+ZS^A_{\rm inc}(Q)\,]\ . \tag{18}$$

The form factor and incoherent scattering factor were obtained on the basis of the Thomas-Fermi model of a cold atom, i.e., the same calculation as in the construction of cross-section tables.[12]

The results of Fig. 1 indicate that the x-ray-scattering cross section undergoes large changes in both angular distribution and in absolute value with the increase in plasma temperature. The major contribution to the scattering cross section for the cold target at angles less than 60° is due to coherent scattering. At 150 eV this effect decreases since the product of the coherent scattering cross section for the 12.4 bound electrons times the ion-ion structure factor for the momentum change associated with the scattering angle becomes significantly smaller (see Ref. 5). At angles greater than 90° the scattering is still dominated by coherent scattering, however, the difference in this process between the 150-eV plasma and the cold material decreases. The ion-ion structure factor for these angles is essentially unity for the 150-eV plasma. In the region between 0° and 10° the major contribution to the scattering is due to the free-electron term, Eqs. (16) and (17).

Two relatively low-temperature carbon plasmas were studied here, the first at a density of 0.1 g/cm^3 and temperature of 2 eV while the density and temperature of the second plasma were 5.4 g/cm^3 and 13 eV, respectively. The number of bound electrons in the first plasma is 5.0 and the plasma parameter is $\Gamma=2$. In the second plasma these values are 3.0 and 10, respectively, and the free-electron coupling parameter in both cases is approximately 2. As mentioned above the radial distribution functions for both ions and electrons in both these plasmas were assumed to be given by the OCP model. The ion structure factors which have a decisive effect on the scattering are plotted as a function of scattering angle for both these carbon plasmas in Fig. 2. The assumption of using the OCP model for the ion radial distribution will be discussed below.

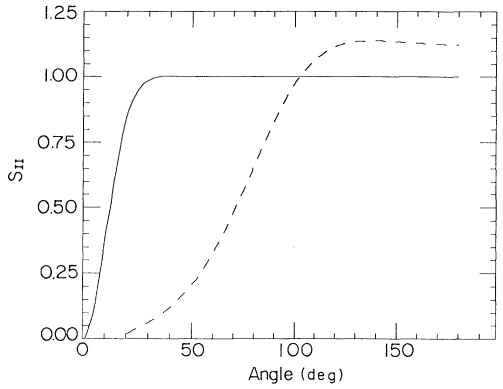

FIG. 2. Ion-ion structure factors as a function of scattering angle for carbon plasma at incident x-ray energy of 5 keV. Solid curve for plasma at 2 eV and density of 0.1 g/cm^3, dashed curve 13-eV plasma at density of 5.4 g/cm^3.

In Fig. 3 are plotted the bound-electron form factors [Eq. (5)] times the Thompson scattering cross section for both plasmas as well as for cold carbon, which in the latter case gives the coherent scattering cross section. In the case of the plasma studied here the degree of ionization increases with temperature. The radial distribution of the bound electrons thus contracts as the temperature increases. Since the form factor is essentially the Fourier transform of the bound-electron radial distribution function, it broadens as the temperature increases. The value

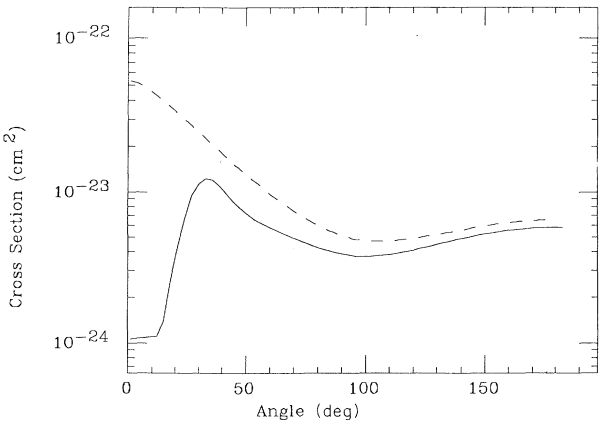

FIG. 1. Total scattering cross section as a function of angle for 10-keV x rays incident on Fe targets. Top curve, cold Fe at the natural density (dashed curve); bottom curve, Fe at 150 eV and at the natural density (solid curve).

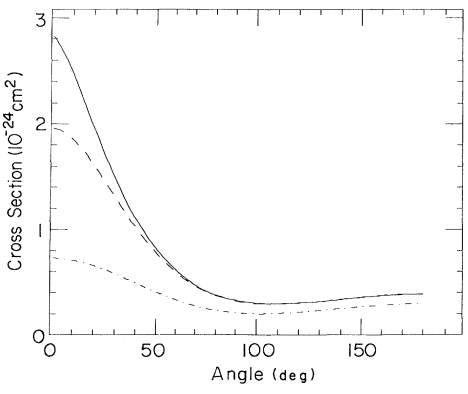

FIG. 3. Bound-electron form factor times classical scattering cross section as a function of scattering angle for 5-keV x rays incident on carbon. Top curve, cold carbon; middle curve, carbon at 2 eV and density 0.1 g/cm^3; bottom curve, carbon at 13 eV and 5.4 g/cm^3.

of the form factor at 0° is determined by the number of bound electrons. The total incoherent scattering cross section from the free and bound electrons in both carbon plasmas studied here does not differ substantially from the incoherent scattering cross section in the cold carbon case. The interference term is small here compared to the coherent and incoherent scattering terms.

In Fig. 4 are given the total scattering cross section for 5-keV x rays for both plasmas discussed above as well as for cold carbon and for a high-temperature, fully ionized carbon plasma. The cross section of the coolest plasma is not much different from the cold carbon with the exception of the interval from 0° to 20°, due to the effect of the ion-ion structure factor. The coherent cross section of the five bound electrons in the plasma for angles greater than 60° is equal to that from the six bound electrons in cold carbon, see Fig. 3. The slight increase in the total cross section at angles greater than 90° in the plasma compared to the cold target is due to the contribution of the total incoherent scattering cross section in the plasma case.

A much more dramatic change between the plasma scattering and the cold carbon cross section is observed for the 13-eV plasma. As in the case of the 150-eV Fe plasma the reduction of the scattering due to the product of the ion-ion structure factor times the coherent scattering cross section dominates the shape of the cross section. The increase in the scattering at the large angles in the plasma state compared to the cold material is due to the contributions of the total incoherent cross section as well as to the interference term. The latter process is not negligible at the large angles; at 180°, for example, the interference term is 70% of the coherent scattering term.

The carbon plasma at 200 eV and density 0.1 g/cm^3 is fully ionized and scattering is due entirely to the free electrons. This plasma is weakly coupled with the ion-ion coupling parameter less than unity and the electron-electron coupling parameter 0.04. The electron-electron structure factor is thus well described by Eq. (16) and is essentially unity with the exception of the region around 0° where the structure factor is 0.86. The total scattering cross section which is given in Fig. 4 is thus close to the classical Thompson scattering cross sections of the free-electrons. The scattering cross sections as a function of angle here are different than for the two cooler carbon plasmas and cold carbon target also plotted in Fig. 4. At angles greater than 90° the cross section in the latter three cases is higher than for the high-temperature carbon plasma due to the coherent scattering which dominates the scattering.

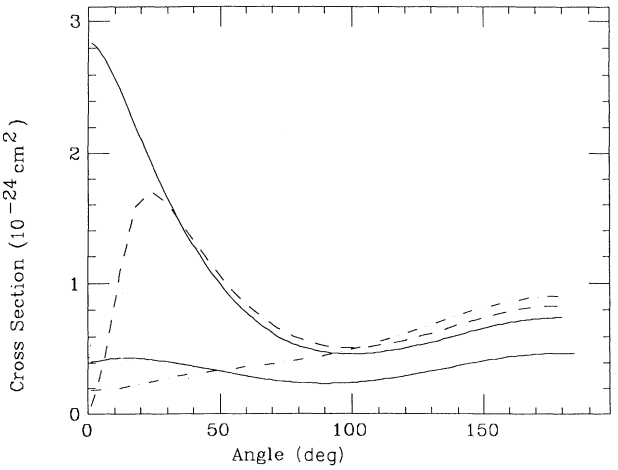

FIG. 4. Total scattering cross section as a function of angle for 5-keV x rays incident on C targets. Top curve, cold C at the natural density (solid curve). Dashed curve, C at 2 eV and density of 0.1 g/cm^3; dot-dashed curve, C at 13 eV and density of 5.4 g/cm^3. Lower solid curve, carbon plasma at 200 eV and 0.1 g/cm^3.

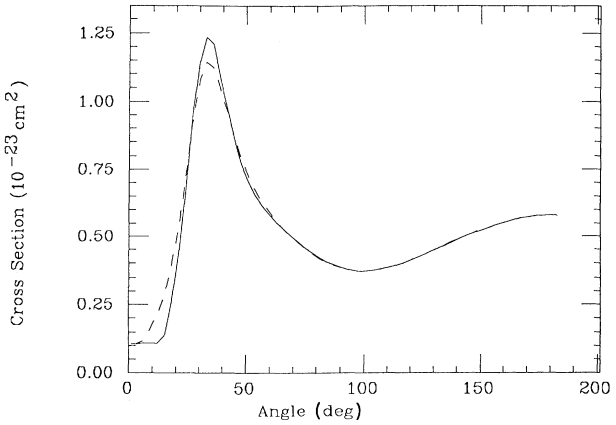

FIG. 5. Angular distribution of scattered 10-keV x rays from an Fe plasma at 150 eV and density of 7.59 g/cm^3 using two different ion-ion structure factors. Dashed curve with the self-consistent result of the HNC–Thomas-Fermi procedure (Ref. 10), while the solid curve is that using the OCP approximation with $\Gamma = 10$.

Some insight into the validity of the OCP approximation for the ion radial distribution function could be gained by comparing the calculated scattering cross sections using this distribution to those obtained using the more elaborate HNC-TF procedure. The results for the Fe plasma at 150 eV discussed in the preceding section are compared to the scattering cross section using the OCP radial distribution for $\Gamma = 10$ (the plasma parameter according to the HNC-TF solution is 13.5). The results of the comparison are presented in Fig. 5 where it is seen that the differences between the two distributions are small with the exception of the low values of the cross section in the small angle region. These differences are much less than the magnitude of the gross changes in the scattering cross section stressed in this paper. The same considerations should apply to the weaker coupled carbon plasma where we do not at this stage possess a self-consistent distribution of the ion structure factor.

DISCUSSION

We have proposed a procedure for calculating the x-ray-scattering cross section from hot dense plasma, which contains free and bound electrons for x rays in the kilo-

electron-volt range. The method follows that used for liquid metals[6] where the free and bound electrons in the plasma case correspond to the valence and core electrons of the liquid metal.

Basic to the calculation of the scattering cross section are the bound-electron radial distribution, the ion-ion structure factor, the ion–free-electron structure factor, and the free-electron structure factor. The first three were determined from the solution of the Thomas-Fermi model in the correlation sphere where both ions and electrons were accounted for. In one case the ion-ion structure factor was calculated self-consistently while in two other cases the OCP model was assumed. The free-electron structure factor was calculated in the weak-coupling limit assuming Debye-Hückel theory. This assumption is valid for the high-temperature carbon plasma where the free-electron scattering dominates the cross section. The accuracy of this assumption in the other cases is not as good, however, here free-electron scattering is of minor influence.

The results of the calculations indicate that significant changes in the x-ray-scattering cross section in both intensity and shape are obtained in the plasma state compared to cold matter at standard conditions. Such changes are also observed between different plasma conditions characterized by temperature and density. Iron plasmas at 150 eV and at the natural density were studied and compared to cold iron; these results are depicted in Fig. 1. Carbon plasmas at significantly lower temperatures were studied; here we cite in particular the 13 eV, 5.4 g/cm^3 plasma which gives a drastically different angular distribution compared to the cold carbon target; see Fig. 4. As pointed out above, such plasma could currently be produced in the laboratory[2] and could be diagnosed by scattering a short duration x-ray burst of several keV from the above-mentioned plasma.

Improved modeling of the ion-ion structure factor as well as for the free-electron structure factor are planned to be pursued in future work. In this manner the sensitivity of this method as a diagnostic tool could be investigated. Finally, comparison to experiment could elucidate the validity of the calculational procedure and in particular the validity of the physical models used in the calculation.

[1]J. Oliva and R. M. More, UCRL Report No. UCRL-50021-84, pp. 3–71, 1984 (unpublished).
[2]R. Riley, O. Willi, S. J. Rose, and T. Afshar-Rad, Europhys. Lett. **10**, 135 (1989).
[3]O. Theimer, Phys. Lett. **20**, 39 (1966).
[4]D. B. Boercker, R. W. Lee, and F. J. Rogers, J. Phys. B **16**, 3279 (1983).
[5]E. Nardi, Y. Rosenfeld, and D. Ofer, J. Phys. (Paris) Colloq. **49**, C7-267 (1988).
[6]J. Chihara, J. Phys. F **17**, 295 (1987).
[7]C. Deutsch, J. Non-Cryst. Solids **8**, 713 (1972); H. Minoo, C. Deutsch, and J. P. Hansen, Phys. Rev. A **14**, 840 (1976).
[8]J. Chihara, J. Phys. C **18**, 3103 (1985).
[9]N. W. Ashcroft and D. Stroud, in *Solid State Physics: Advances in Research and Applications,* edited by H. Ehrenreich, F. Seitz, and D. Turnbull (Academic, New York, 1988), Vol. 33, p. 1.
[10]D. Ofer, E. Nardi, and Y. Rosenfeld, Phys. Rev. A **38**, 5801 (1988).
[11]L. B. Mendelsohn and F. Biggs, Phys. Rev. A **5**, 688 (1971).
[12]W. D. Brown, Boeing Report No. D2-125137-1, 1966 (unpublished).
[13]D. B. Boercker and R. M. More, Phys. Rev. A **33**, 1859 (1986).
[14]E. E. Salpeter, J. Geophys. Res. **68**, 1321 (1963).